Online Appendix to Optimal Carbon Abatement in a Stochastic Equilibrium Model with Climate Change

Christoph Hambel[a], Holger Kraft[b,*], Eduardo Schwartz[c]

[a,b] *Goethe University Frankfurt, Faculty of Economics and Business Administration, Theodor-W.-Adorno-Platz 3, 60323 Frankfurt am Main, Germany.*
[c] *UCLA Anderson School of Management, Los Angeles.*

This version: December 22, 2020

Abstract

This online appendix contains additional robustness checks and a description of the numerical solution method.

---

* Corresponding author. Phone: +49 69 798 33699.

E-mail addresses: christoph.hambel@finance.uni-frankfurt.de (Christoph Hambel), holgerkraft@finance.uni-frankfurt.de (Holger Kraft), eduardo.schwartz@anderson.ucla.edu (Eduardo Schwartz)

Preferences	2015	2035	2055	2075	2095	2115	2150	2200
Benchmark	11.12	21.75	50.67	102.52	171.21	225.10	254.12	353.25
DICE	7.67	14.03	35.15	77.01	137.83	201.57	243.49	324.95
Stern	38.11	77.30	139.02	185.47	208.60	223.44	250.53	377.84

Table 13: SCC for Different Preference Specifications. The table compares SCC [$/tCO$_2$] for different preference specifications. The results are generated using the (G-N) damage specification. DICE preferences are $\gamma = 1.45$, $\psi = 1/\gamma$, $\delta = 1.5\%$. Stern refers to $\gamma = 1$, $\psi = 1$, $\delta = 0.1\%$.

E Further Robustness Checks

E.1 Negative Net Emissions

This section studies a situation where negative net emissions are allowed to some extent. For this purpose, we restrict the emission control rate between 0 and 1.2, i.e., we allow for negative emissions of up to 20% of BAU emissions, which is in line with Nordhaus (2017). The main results are virtually unaffected by this assumption. The main difference is that the tight abatement constraint imposed in the main text makes it harder to make up for opportunities that were missed in the past. Therefore, if negative emissions are possible, society slightly delays abatement activities. This effect already kicks in for moderate damages: For the Nordhaus damage specification (L-N), the initial SCC is approximately 3% lower than in the benchmark case, where negative emissions are not allowed. In the year 2115, however, the median SCC increases by 4% and the 95% quantile of SCC is 11% higher than in the benchmark case. In extreme paths with high temperatures, society must act much more drastically and reduces emissions below zero, which boosts the SCC in such a situation. If damages are severe, this effect is much more pronounced since extreme paths involves even stronger damages. For instance, in the Weitzman damage specification (L-W), the initial SCC is 31% smaller. In the year 2115, the median SCC increases by 11% and the 95% quantile of SCC is 17% higher than in the benchmark case.

E.2 Comparison with Standard Preference Choices

We now compare our benchmark preference structure with two specifications that are standard in the literature. First, we consider a time-additive CRRA utility function with a risk aversion parameter of $\gamma = 1.45$ and time-preference rate of $\delta = 1.5\%$. This utility specification is used as benchmark specification in DICE. Earlier versions and other models use similar CRRA specifications.[42] Second, we simulate our model using a log-utility function ($\psi = \gamma = 1$) with a very low discount rate ($\delta = 0.1\%$). Pindyck (2013), among others, argues that optimal abatement policies crucially depend on the time-preference rate. In general, there is a lot of debate about this parameter in the IAM literature. This is because time-preferences put implicitly weights on

[42] See, e.g., Nordhaus (2008), Pindyck (2012), Ackerman et al. (2011).

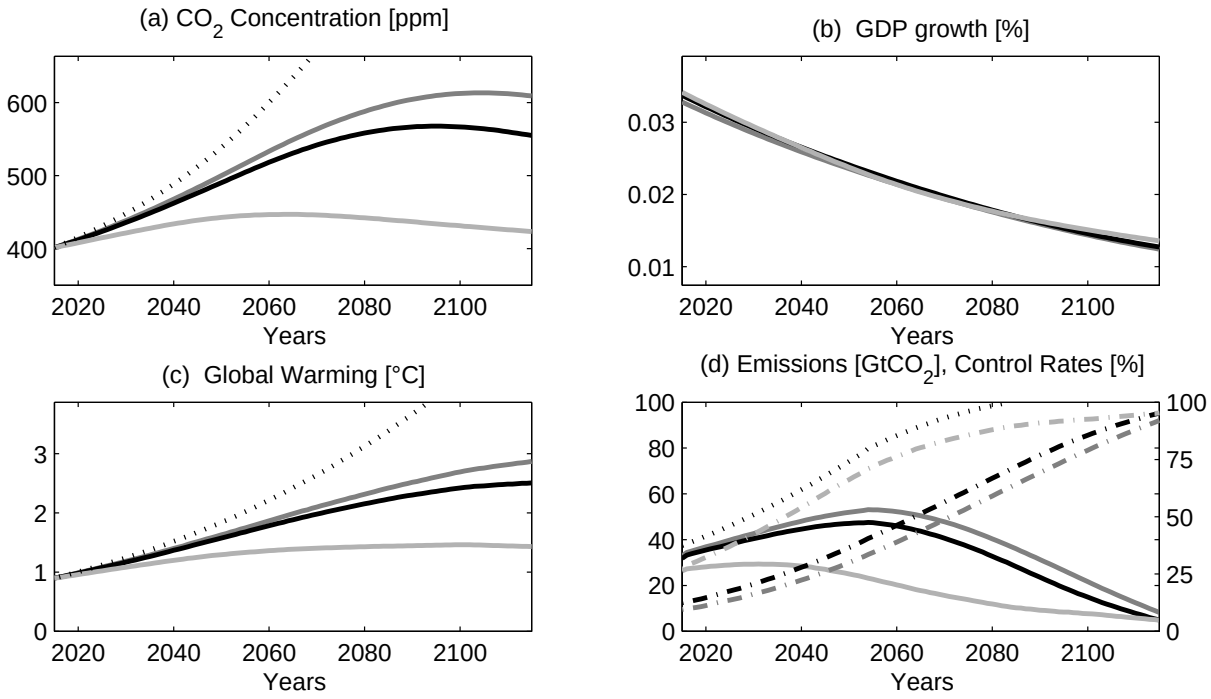

Figure 11: Sensitivity Analysis for the Preferences. The graphs show the median paths of the key variables for different preference specifications. Median optimal paths are depicted by solid lines and median BAU paths by dotted lines. The benchmark scenario is depicted by black lines. Grey lines show the DICE preference structure and light lines represent Stern discounting. Graph (a) shows the carbon dioxide concentrations in the atmosphere, (b) median GDP growth rates, (c) median changes in global temperature, (d) carbon dioxide emissions and the optimal emission control rates (dash-dotted lines).

the current and future generations: A higher value puts more weight on the current generation, whereas a lower value shifts some of this weight to future generations. A tension arises since the current generation is not as severely affected by the climate change as the future generations, but must today decide upon an optimal abatement policy and pay for it. Of course, more stringent actions reduce current consumption, but have far reaching consequences for future generations who might benefit the most. We refer to the very low discount rate of $\delta = 0.1\%$ in combination with log-utility as *Stern discounting* since Stern (2007) suggests this preference structure. Intuitively, with such a low rate of time-preference, real interest rates are lower and, in turn, the social cost of carbon is higher. This also implies that society implements a very stringent abatement policy.

Table 13 and Figure 11 summarizes our findings on how the preference structure affects our results. With the standard DICE preference structure, both risk aversion and EIS are lower which leads to a moderate abatement policy. The resulting evolution of median global warming is in line with the results presented in Nordhaus and Sztorc (2013) although SCC is significantly smaller. *Stern discounting* yields a very stringent abatement policy and a high social cost of carbon. Following this policy reduces carbon dioxide emissions so that the median temperature

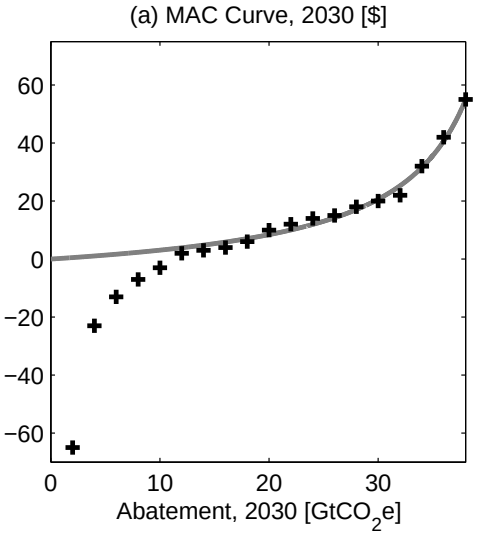

Figure 12: Calibration of the Abatement Costs. The figure depicts the marginal abatement cost (MAC) for the reference year 2030 (solid line). The prices of the y-axis are in 2005 euros. $GtCO_2e$ stands for gigatons of carbon dioxide equivalents. The MAC function is calibrated such that it fits the positive part of the McKinsey data (crosses).

increase peaks by the end of this century at 1.5°C. Additionally, climate variability is significantly dampened (not shown in the figure).

E.3 Alternative Abatement Costs

We now study the effects of using an alternative cost function κ. Instead of the benchmark specification, we derive an abatement cost function using the prognosis for the marginal greenhouse gas abatement costs for the year 2030 provided by McKinsey and Company (2009, 2010).

Calibration The calibration is based on a prognosis for the marginal greenhouse gas abatement costs for the year 2030 provided by McKinsey and Company (2009, 2010). For that year, they estimate that under BAU the total emissions of greenhouse gases would reach $66GtCO_2e$ and analyze the expected abatement expenditures. Under rather optimistic assumptions, they report an abatement potential of $38GtCO_2e$ at a total cost of 150 billion euros. McKinsey supposes that for $11GtCO_2e$ of abatement the net costs are negative because savings from implementing energy-efficient measures – compared to the BAU scenario – exceed the initial investment costs. To avoid issues arising from negative abatement costs, we follow Ackerman and Bueno (2011) and disregard the negative part of the marginal costs. Therefore, our calibration is more conservative than the McKinsey prognosis.

In a first step, we fit the McKinsey data using the following functional form for the marginal abatement cost function:

$$\mathrm{MAC}(q) = \frac{c_1 q}{c_2 + c_3 q + c_4 q^2}.$$

The variable q is the absolute quantity of greenhouse gas abatement (measured in $GtCO_2$) compared to the business-as-usual scenario, i.e., the difference between BAU-emissions and controlled emissions, $q = E^{\mathrm{BAU}} - E$. As can be seen in Figure 12, our estimates of c_i fit the positive part of the marginal abatement costs well ($R^2 > 0.96$). The coefficients are $c_1 = 0.00039$, $c_2 = 0.0016$, $c_3 = -3.25 \cdot 10^{-5}$, $c_4 = -7.27 \cdot 10^{-8}$. Then, we transform the marginal costs MAC into (absolute) expenditures, which in our paper are denoted by X. We thus compute the anti-derivative $X(q)$ of the marginal costs with respect to q and evaluate X at the available data points $q_1, \ldots, q_n$. This yields values $X_1, \ldots, X_n$.

The resulting data points $(q_1, X_1), \ldots, (q_N, X_N)$ can now be used to determine the cost function $\kappa(t, \varepsilon)$ for the year 2030. Notice that the McKinsey data maps absolute quantities of abatement q into marginal expenditures, whereas our cost function maps emission control rates into reductions of economic growth. Therefore, we transform absolute quantities of greenhouse gas abatement q into emission control rates using $\varepsilon_i = q_i / E^{\mathrm{BAU}}$, $i = 1, \ldots, N$, and absolute abatement expenditures X in relative expenditures by $\varkappa_i = X_i / \mathbb{E}[Y]$, $i = 1, \ldots, N$, where $\mathbb{E}[Y]$ denotes the expected GDP in 2030. We assume the functional form (24) still to hold. We calibrate the parameters such that (24) is close to the data points $(\varepsilon_1, \varkappa_1), \ldots, (\varepsilon_N, \varkappa_N)$. As a result of the calibration we obtain $a = 0.035$, $b = 3.186$ ($R^2 > 99\%$) for the year 2030. We take the rate at which abatement becomes cheaper over time from DICE, i.e. the relative expenditures for complete abatement ($\varepsilon = 1$) decline at rate of 1.48% to its long-term level of 0.043%. As a result, we obtain $a(t) = 0.0443 \exp(-0.0148t) + 0.00043$. Notice that the calibration based on the McKinsey prognosis makes abatement slightly cheaper than in DICE since b is smaller.

Results for (G-N) Figure 13 depicts the median results for both cost specifications and (G-N).[43] It turns out that the results are similar. Implementing the McKinsey specification, slightly raises the optimal abatement policy leading to lower carbon dioxide concentrations and temperatures compared to the benchmark case. Therefore, net GDP growth is slightly higher and SCC in the year 2015 is reduced from \$11.12 to \$10.05. Notice that, by the end of this century, the optimal abatement activity becomes higher for the DICE cost function. This is because for high emission control rates the marginal costs of the McKinsey calibration are higher than for DICE since θ_2 is higher (3.186 instead of 2.8). In turn, the marginal benefits from abatement are lower when control rates are high.

[43] The results for (L-N) are similar and available from the authors upon request.

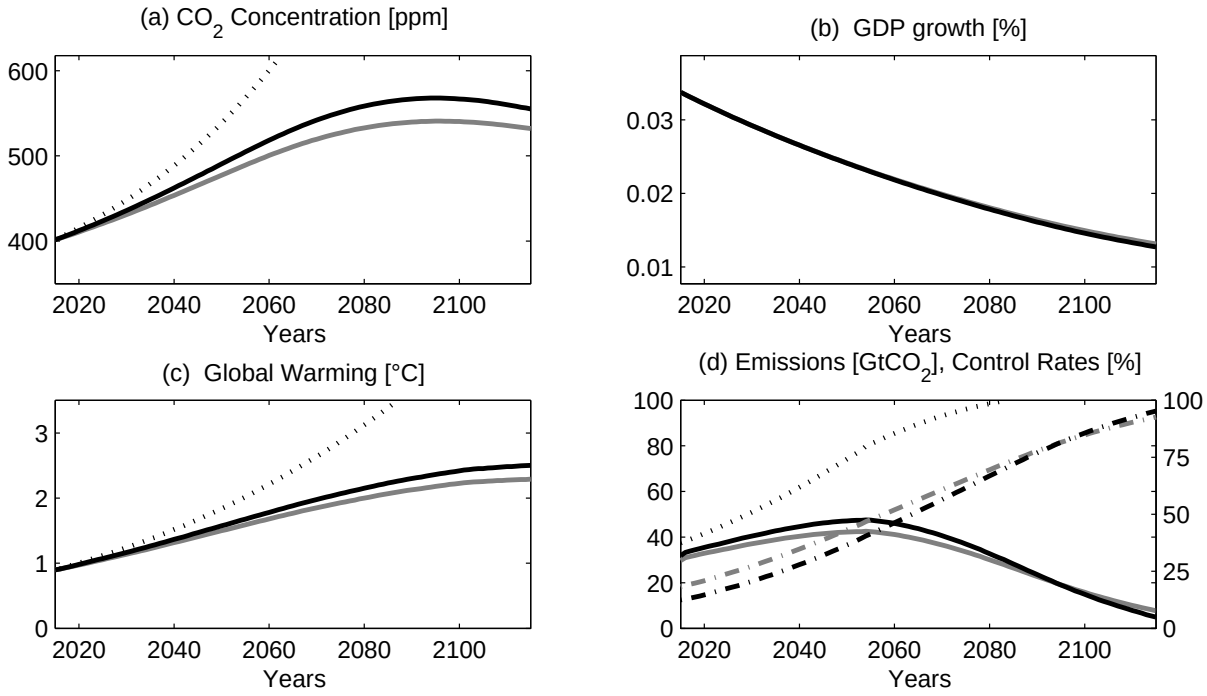

Figure 13: Sensitivity Analysis for the Cost Function. The graphs show the median paths of the key variables for different specifications of the cost function. Median optimal paths are depicted by solid lines and median BAU paths by dotted lines. The benchmark scenario is depicted by black lines. Grey lines show the results using McKinsey abatement costs. Graph (a) shows the carbon dioxide concentrations, (b) median GDP growth rates, (c) median changes in global temperature, (d) carbon dioxide emissions and the optimal emission control rates (dash-dotted lines).

F Solution Method

The optimization problem (16) cannot be solved explicitly.[44] This appendix summarizes how the problem can be solved numerically.

F.1 Hamilton-Jacobi-Bellman Equation

In case of a growth rate impact, the Hamilton-Jacobi-Bellman (HJB) equation reads

$$0 = \sup_{\alpha,\chi}\Big\{ V_t + y\big(g(t,\chi) - \zeta_d\tau^n - \kappa(t,\varepsilon)\big)V_y + \frac{1}{2}y^2\sigma_k^2 V_{yy} + m(g_m(t)-\alpha)V_m + \frac{1}{2}m^2\sigma_m^2 V_{mm} \\ - \delta_m(m^s)mV_{m^s} + \frac{m\eta_\tau}{m+M^{\mathrm{PI}}}\big(g_m(t)-\alpha\big)V_\tau + \frac{1}{2}\Big(\frac{\sigma_\tau m}{m+M^{\mathrm{PI}}}\Big)^2 V_{\tau\tau} + \frac{m^2}{m+M^{\mathrm{PI}}}\rho_{m\tau}\sigma_m\sigma_\tau V_{m\tau}$$

[44] Notice that closed-form solutions are only available in rare special cases. A prominent example is the combination of log-utility, a Cobb-Douglas production technology and some further debatable assumptions as in Golosov et al. (2014). As discussed in Section 5, log-utility is too restrictive for studying the effects of preference parameters.

$$+ ym\rho_{km}\sigma_k\sigma_m V_{ym} + y\sigma_k\rho_{k\tau}\frac{\sigma_\tau m}{m+M^{\mathrm{PI}}}V_{y\tau} + \pi_\tau(\tau)\big[V(t,y,m,m^s,\tau+\theta_\tau) - V\big] + f(\chi y, V)\Big\}. \tag{25}$$

Subscripts of the indirect utility function V denote partial derivatives (e.g., $V_t = \partial V/\partial t$). The corresponding HJB equation for a level impact can be found in Section F.3. First, we establish the following separation result:

Lemma F.1. *The indirect utility function of the optimization problem (16) has the form*

$$V(t,y,m,m^s,\tau) = \frac{1}{1-\gamma}y^{1-\gamma}F(t,m,m^s,\tau), \tag{26}$$

where F solves the simplified HJB equation

$$\begin{aligned} 0 = \sup_{\alpha,\chi}\Big\{ & F_t + m\big[g_m(t) - \alpha + (1-\gamma)\sigma_k\sigma_m\rho_{km}\big]F_m + \frac{1}{2}m^2\sigma_m^2 F_{mm} + \delta_m(m^s)mF_{m^s} \\ & + \frac{m\eta_\tau}{m+M^{\mathrm{PI}}}\big[g_m(t) - \alpha + (1-\gamma)\rho_{k\tau}\sigma_k\sigma_\tau\big]F_\tau + \frac{1}{2}\Big(\frac{m\sigma_\tau}{m+M^{\mathrm{PI}}}\Big)^2 F_{\tau\tau} \\ & + \frac{m^2}{m+M^{\mathrm{PI}}}\rho_{m\tau}\sigma_m\sigma_\tau F_{m\tau} + (1-\gamma)\Big[g(t,\chi) - \zeta_d\tau - \kappa(t,\varepsilon^\alpha) - \frac{1}{2}\gamma\sigma_k^2 - \frac{\delta}{1-1/\psi}\Big]F \\ & + \pi_\tau(\tau)\big[F(t,m,m^s,\tau+\theta_\tau(\tau)) - F\big] + \delta\theta\chi^{1-1/\psi}F^{1-1/\theta}\Big\}, \end{aligned} \tag{27}$$

The optimal abatement strategy is given by

$$\alpha_t^* = \kappa_\alpha(t,m,\cdot)^{-1}\left(\frac{mF_m + \frac{m\eta_\tau}{m+M^{\mathrm{PI}}}F_\tau}{(\gamma-1)F}\right), \tag{28}$$

and the optimal consumption rate satisfies

$$\delta(\chi_t^*)^{-1/\psi}F^{-1/\theta} = -\frac{\partial}{\partial\chi}g(t,\chi_t^*). \tag{29}$$

Proof. Substituting the conjecture into the HJB equation yields the simplified HJB equation (27). The representations of the optimal controls are then obtained by calculating the first-order conditions. □

The HJB equation cannot be simplified further. Therefore, we have to determine F by solving equation (27) numerically. First, we consider a simplified problem where the capacity of natural sinks is assumed to be unconstrained, i.e., the decay rate of carbon dioxide is assumed to be constant at $\overline{\delta}_m = \delta_m(0)$. This provisional assumption makes the state variable M^s redundant and significantly simplifies the solution algorithm. In a second step, we address the general case.

F.2 Numerical Solution Approach

Basic Idea We use a grid based solution approach to solve the non-linear PDE. We discretize the (t, m, τ)-space using an equally spaced lattice. Its grid points are defined by

$$\big\{(t_n, m_i, \tau_j) \mid n = 0, \cdots, N_t,\, i = 0, \cdots, N_m,\, j = 0, \cdots, N_\tau\big\},$$

where $t_n = n\Delta_t$, $m_i = i\Delta_m$, and $\tau_j = j\Delta_\tau$ for some fixed grid size parameters Δ_t, Δ_m, and Δ_τ that denote the distances between two grid points. The numerical results are based on a choice of $N_m = 500$, $N_\tau = 1000$ and 1 time step per year. Our results hardly change if we use a finer grid or more time steps per year. The parameters N_τ and N_m are chosen sufficiently large such that it is very unlikely that these boundaries are reached within the given time horizon. In the sequel, $F_{n,i,j}$ denotes the approximated indirect utility function at the grid point (t_n, m_i, τ_j) and $\alpha_{n,i,j}$ refers to the corresponding optimal abatement policy. We apply an implicit finite difference scheme.

Terminal Condition Since the optimization problem (16) has an infinite time horizon, we must transform it into a problem with a finite horizon. Therefore, we approximate the indirect utility function at some point $t_{\max} = N_t\Delta_t$ in the distant future – we choose the year 2500 – by the solution of a similar problem where the world is in a steady state: We assume that from time $t_{\max}$ onwards the emission control rate is one, i.e., anthropogenic carbon dioxide emissions are zero. To approximate the indirect utility function at the grid point $(t_{\max}, m_i, \tau_j)$, we simulate sample paths for further 500 years and determine the utility index (14).

Finite Differences Approach In this paragraph, we describe the numerical solution approach in more detail. We adapt the numerical solution approach used by Munk and Sørensen (2010).

The numerical procedure works as follows. At any point in time, we make a conjecture for the optimal abatement policy $\alpha^*_{n,i,j}$. A good guess is the value at the previous grid point since the abatement strategy varies only slightly over a small time interval, i.e., we set $\alpha^*_{n,i,j} = \alpha_{n+1,i,j}$. Substituting this guess into the HJB equation yields a semi-linear PDE:

$$0 = F_t + K_1 F^{1-\frac{1}{\theta}} + K_2 F + K_3 F_m + K_4 F_{mm} + K_5 F_\tau + K_6 F_{\tau\tau} + K_7 F_{\tau m} + \pi_\tau F(t, m, \tau + \theta_\tau)$$

with state dependent coefficients $K_i = K_i(t, m, \tau)$. Due to the implicit approach, we approximate the time derivative by forward finite differences. In the approximation, we use the so-called

'up-wind' scheme that stabilizes the finite differences approach. Therefore, the relevant finite differences at the grid point (n, i, j) are given by

$$\begin{aligned}
\mathrm{D}_m^+ F_{n,i,j} &= \frac{F_{n,i+1,j} - F_{n,i,j}}{\Delta_m}, \qquad \mathrm{D}_m^- F_{n,i,j} = \frac{F_{n,i,j} - F_{n,i-1,j}}{\Delta_m}, \\
\mathrm{D}_\tau^+ F_{n,i,j} &= \frac{F_{n,i,j+1} - F_{n,i,j}}{\Delta_\tau}, \qquad \mathrm{D}_\tau^- F_{n,i,j} = \frac{F_{n,i,j} - F_{n,i,j-1}}{\Delta_\tau}, \\
\mathrm{D}_{mm}^2 F_{n,i,j} &= \frac{F_{n,i+1,j} - 2F_{n,i,j} + F_{n,i-1,j}}{\Delta_m^2}, \qquad \mathrm{D}_{\tau\tau}^2 F_{n,i,j} = \frac{F_{n,i,j+1} - 2F_{n,i,j} + F_{n,i,j-1}}{\Delta_\tau^2} \\
\mathrm{D}_t^+ F_{n,i,j} &= \frac{F_{n+1,i,j} - F_{n,i,j}}{\Delta_t}, \qquad \mathrm{D}_{\tau y}^2 F_{n,i,j} = \frac{F_{n,i,j+1} - F_{n,i-1,j+1} - F_{n,i+1,j-1} + F_{n,i-1,j-1}}{4\Delta_\tau \Delta_m}.
\end{aligned}$$

We approximate the jump terms via linear interpolation between the closest grid points:

$$F(t, m, \tau + \theta_\tau) = k_{\tau 1} F_{n,i,j+\widehat{\theta}_{\tau 1}} + k_{\tau 2} F_{n,i,j+\widehat{\theta}_{\tau 2}},$$

where $\widehat{\theta}_{\tau 1}$ and $\widehat{\theta}_{\tau 2}$ denote the closest grid points of $\tau + \theta_\tau$. The variables $k_{\tau\cdot}$ denote the weights resulting from linear interpolation. Substituting these expressions into the PDE above yields the following semi-linear equation for the grid point (t_n, m_i, τ_j)

$$\begin{aligned}
F_{n+1,i,j} \frac{1}{\Delta_t} &= F_{n,i,j} \left[-K_2 + \frac{1}{\Delta_t} + \mathrm{abs}\left(\frac{K_3}{\Delta_m}\right) + \mathrm{abs}\left(\frac{K_5}{\Delta_\tau}\right) + 2\frac{K_4}{\Delta_m^2} + 2\frac{K_6}{\Delta_\tau^2} \right] \\
&+ F_{n,i-1,j} \left[\frac{K_3^-}{\Delta_m} - \frac{K_4}{\Delta_m^2} \right] + F_{n,i+1,j} \left[-\frac{K_3^+}{\Delta_m} - \frac{K_4}{\Delta_m^2} \right] \\
&+ F_{n,i,j-1} \left[\frac{K_5^-}{\Delta_\tau} - \frac{K_6}{\Delta_\tau^2} \right] + F_{n,i,j+1} \left[-\frac{K_5^+}{\Delta_\tau} - \frac{K_6}{\Delta_\tau^2} \right] \\
&+ F_{n,i-1,j+1} \frac{K_7}{4\Delta_\tau \Delta_m} + F_{n,i+1,j-1} \frac{K_7}{4\Delta_\tau \Delta_m} - F_{n,i+1,j+1} \frac{K_7}{4\Delta_\tau \Delta_m} - F_{n,i-1,j-1} \frac{K_7}{4\Delta_\tau \Delta_m} \\
&+ \pi_\tau (k_{\tau 1} F_{n,i,j+\widehat{\theta}_{\tau 1}} + k_{\tau 2} F_{n,i,j+\widehat{\theta}_{\tau 2}}) - K_1 F_{n,i,j}^{1-\frac{1}{\theta}}.
\end{aligned}$$

Therefore, for a fixed point in time each grid point is determined by a non-linear equation. This results in a non-linear system of $(N_m + 1)(N_\tau + 1)$ equations that can be solved for the vector

$$F_n = (F_{n,1,1}, \cdots, F_{n,1,N_\tau}, F_{n,2,1}, \cdots, F_{n,2,N_\tau}, \cdots, F_{n,N_m,1}, \cdots, F_{n,N_m,N_\tau}).$$

Notice that in case of CRRA utility the system becomes linear. Using this solution we update our conjecture for the optimal abatement policy at the current point in the time dimension. We apply the first-order condition (28) and finite difference approximations of the corresponding derivatives. In the interior of the grid, we use centered finite differences. At the boundaries, we

apply forward or backward differences. For instance, for $(i,j) \in \{2,\dots,N_m-1\}\times\{2,\dots,N_\tau-1\}$, we compute the new guess as

$$\alpha^*_{n,i,j} = \kappa_\alpha(t_n, m_i, \cdot)^{-1}\left(\frac{(m_i + M^{\mathrm{PI}})\Delta_\tau m_i(F_{n,i+1,j} - F_{n,i-1,j}) + \Delta_m m_i(F_{n,i,j+1} - F_{n,i,j-1})}{\Delta_m\Delta_\tau(m_i + M^{\mathrm{PI}})(\gamma-1)F_{n,i,j}}\right).$$

Similarly, we compute the social cost of carbon for fixed GDP Y in the grid point $(i,j) \in \{2,\dots,N_m-1\}\times\{2,\dots,N_\tau-1\}$ as

$$\mathrm{SCC}_{n,i,j} = \frac{Y}{1-\gamma}\frac{F_{n,i+1,j} - F_{n,i-1,j}}{\Delta_m F_{n,i,j}}\frac{\xi_{\mathfrak{e}}}{\mu_m + \delta_m - \alpha^*_{n,i,j}}.$$

With this new guess for the optimal policy we perform a new iterative step. We continue the iteration until there is no significant change of the result. Then the algorithm continues with the previous point t_{n-1} in the time directions until we reach the end of the grid.

Implementation of State-Dependent Sinks The solution procedure described so far does not deal with state dependent sinks. Since in general the constraint (21) involves M^s, we first solve for the optimal abatement policy if the weaker constraint $\alpha_t \le g_m(t) + \overline{\delta}_m$ is imposed. The corresponding abatement decision is then given by

$$\overline{\alpha}_t = \min\left[g_m(t) + \overline{\delta}_m,\ \kappa_\alpha(t,m,\cdot)^{-1}\left(\frac{mF_m + \frac{m\eta}{m+M^{\mathrm{PI}}}F_\tau}{(1-\gamma)F}\right)\right].$$

Since the modified constraint is always weaker, we obtain an upper bound $\overline{J}(t,y,m,m^s,\tau) \ge J(t,y,m,m^s,\tau)$ for the indirect utility function of the true model where (21) is imposed. Of course, $\overline{\alpha}_t$ is not feasible in the true model. To obtain a feasible strategy, we thus define

$$\underline{\alpha}_t = \min\left[g_m(t) + \delta_m(M^s_t),\ \overline{\alpha}_t\right],$$

where we cut off $\overline{\alpha}_t$ if it violates (21). Notice that the strategy $\underline{\alpha}_t$ is suboptimal. Since we have the upper bound $\overline{J}$, we can compute an upper bound on the loss that occurs if we implement $\underline{\alpha}_t$ instead of the (unknown) optimal strategy. If $\underline{J}(t,y,m,m^s,\tau)$ denotes the indirect utility associated with $\underline{\alpha}_t$, the upper bound on the welfare loss is given by

$$\underline{J}(t,y,m,m^s,\tau) = \overline{J}(t,y(1-L),m,m^s,\tau).$$

It turns out that this upper bound for the welfare loss is significantly below 0.1% and thus the strategy $\underline{\alpha}_t$ is close to optimal.

Comparison with Value Function Iteration Most IAMs are formulated in discrete time. The corresponding Bellman equation is usually solved by dynamic programming with value function iteration (see, e.g., Crost and Traeger 2014; Traeger 2014; Cai and Lontzek 2015). The main idea is as follows: One first discretizes the state space and chooses an appropriate functional form to approximate the value function in those nodes. A typical choice are multivariate orthogonal polynomials (e.g., Chebychev polynomials). Starting from the terminal date, one iterates backwards through time. For every t_n one pointwise maximizes the right-hand side of the Bellman equation and determines the approximate value function in every node. Then the algorithm goes step-by-step back in time until the end of the time grid is reached.

Since our model is formulated in continuous time, we derive and solve the corresponding Hamilton-Jacobi-Bellman equation. This partial differential equation can be solved numerically by a grid-based finite-differences approach as described above. Our method is thus the continues-time analogue to discrete-time value function iteration. Notice that it is not necessary to make any assumptions on the functional form of the value function.

F.3 Level Impact

Now, the dynamics of output dynamics are more involved than in the growth rate impact. It is thus more convenient to use $\widehat{Y} = A\widehat{K}$ as a state variable rather than Y. Its dynamics are given by

$$\mathrm{d}\widehat{Y}_t = \widehat{Y}_t \Big[(g(t,\chi_t) - \kappa(t,\varepsilon_t^\alpha))\mathrm{d}t + \sigma_k(\rho_{km}\mathrm{d}W_t^m + \widehat{\rho}_{k\tau}\mathrm{d}W_t^\tau + \widehat{\rho}_k \mathrm{d}W_t^k) \Big]$$

and output is thus

$$Y = \widehat{Y}\, D(T_t).$$

Then, the HJB equation reads

$$\begin{aligned} 0 = \sup_{\alpha,\chi} \Big\{ & V_t + \widehat{y}\,(g(t,\chi) - \kappa(t,\varepsilon^\alpha))\, V_{\widehat{y}} + \frac{1}{2}\widehat{y}^2\sigma_k^2 J_{\widehat{y}\widehat{y}} + m(g_m(t)-\alpha)V_m + \frac{1}{2}m^2\sigma_m^2 J_{mm} \\ & - \delta_m(m^s)mV_{m^s} + \widehat{y}m\rho_{km}\sigma_k\sigma_m V_{\widehat{y}m} + \frac{m\eta_\tau}{m+M^{\mathrm{PI}}}\big(g_m(t)-\alpha\big)V_\tau + \frac{1}{2}\Big(\frac{\sigma_\tau m}{m+M^{\mathrm{PI}}}\Big)^2 V_{\tau\tau} \\ & + \frac{m^2}{m+M^{\mathrm{PI}}}\rho_{m\tau}\sigma_m\sigma_\tau V_{m\tau} + \widehat{y}\sigma_k\rho_{k\tau}\frac{\sigma_\tau m}{m+M^{\mathrm{PI}}}V_{\widehat{y}\tau} + \pi_\tau(\tau)\big[V(t,\widehat{y},m,m^s,\tau+\theta_\tau(\tau)) - V\big] \\ & + f(\widehat{y}D(\tau)\chi, V)\Big\}. \end{aligned}$$

Lemma F.1 is then modified as follows:

Lemma F.2. *The indirect utility function of the optimization problem has the form*

$$J(t,\widehat{y},m,m^s,\tau)=\frac{1}{1-\gamma}\widehat{y}^{1-\gamma}F(t,m,m^s,\tau),$$

where F solves the simplified HJB equation

$$\begin{aligned}0=\sup_{\alpha,\chi}\Big\{&F_t+m\big[g_m(t)-\alpha+(1-\gamma)\sigma_k\sigma_m\rho_{km}\big]F_m+\frac{1}{2}m^2\sigma_m^2F_{mm}+\delta_m(m^s)mF_{m^s}\\&+\frac{m\eta_\tau}{m+M^{\mathrm{PI}}}\big[g_m(t)-\alpha+(1-\gamma)\rho_{k\tau}\sigma_k\sigma_\tau\big]F_\tau+\frac{1}{2}\Big(\frac{m\sigma_\tau}{m+M^{\mathrm{PI}}}\Big)^2F_{\tau\tau}\\&+\frac{m^2}{m+M^{\mathrm{PI}}}\rho_{m\tau}\sigma_m\sigma_\tau F_{m\tau}+(1-\gamma)\Big[g(t,\chi)-\kappa(t,\varepsilon^\alpha)-\frac{1}{2}\gamma\sigma_k^2-\frac{\delta}{1-1/\psi}\Big]F\\&+\pi_\tau(\tau)\big[F(t,m,m^s,\tau+\theta_\tau(\tau))-F\big]+\delta\theta\chi^{1-1/\psi}D(\tau)^{1-1/\psi}F^{1-1/\theta}\Big\},\end{aligned}$$

The optimal abatement strategy is given by

$$\alpha_t^*=\kappa_\alpha(t,m,\cdot)^{-1}\left(\frac{mF_m+\frac{m\eta}{m+M^{\mathrm{PI}}}F_\tau}{(\gamma-1)F}\right)$$

and the optimal consumption rate satisfies

$$\delta(\chi_t^*)^{-1/\psi}F^{-1/\theta}D(\tau)^{1-1/\psi}=-\frac{\partial}{\partial\chi}g(t,\chi_t^*).$$

References

Ackerman, F., and R. Bueno, 2011, Use of McKinsey Abatement Cost Curves for Climate Economics Modeling, *Working Paper,* Stockholm Environment Institute.

Ackerman, F., E. A. Stanton, and R. Bueno, 2011, CRED: A New Model of Climate and Development, *Ecological Economics,* 85, 166–176.

Ackerman, F., E. A. Stanton, and R. Bueno, 2013, Epstein-Zin Utility in DICE: Is Risk Aversion Irrelevant to Climate Policy?, *Environmental and Resource Economics* 56, 73–84.

Aiuppa, A., T. P. Fischer, T. Plank, and P. Bani, 2019, CO_2 flux emissions from the earth's most actively degassing volcanoes, 2005–2015, *Scientific Reports* 9.

Allen, M. R., D. J. Frame, C. Huntingford, C. D. Jones, J. A. Lowe, M. Meinshausen, and N. Meinshausen, 2009, Warming caused by cumulative carbon emissions towards the trillionth tonne, *Nature* 458, 1163–1166.

Bansal, R., D. Kiku, and M. Ochoa, 2014, Climate Change and Growth Risks, *Working Paper,* Duke University.

Bansal, R., and M. Ochoa, 2011, Welfare costs of long-run temperature shifts, *Working Paper,* NBER.

Bansal, R., and A. Yaron, 2004, Risks for the long run: A potential resolution of asset pricing puzzles., *Journal of Finance* 1481–1509.

Barro, R. J., 2006, Rare disasters and asset markets in the twentieth century, *Quarterly Journal of Economics* 121, 823–866.

Barro, R. J., 2009, Rare disasters, asset prices, and welfare costs, *American Economic Review* 99, 243–264.

Burke, M., S. M. Hsiang, and E. Miguel, 2015, Global Non-Linear Effect of Temperature on Economic Production, *Nature* 527, 235–239.

Cai, Y., T. M. Lenton, and T. S. Lontzek, 2016, Risk of multiple interacting tipping points should encourage rapid CO_2 emission reduction, *Nature Climate Change* 6, 520–525.

Cai, Y., and T. S. Lontzek, 2019, The social cost of carbon with economic and climate risks, *Journal of Political Economy* 127, 2684–2734.

Campbell, J. Y., 1999, Asset prices, consumption, and the business cycle, in *J.B: Taylor, M. Woodford (eds.) Handbook of Macroeconomics*, volume 1 (Elsevier North-Holland).

Cox, P. M., C. Huntingford, and M. S. Williamson, 2018, Emergent constraint on equilibrium climate sensitivity from global temperature variability, *Nature* 533, 319–323.

Crost, B., and C. P. Traeger, 2014, Optimal CO2 Mitigation Under Damage Risk Valuation, *Nature Climate Change* 4, 631–636.

Dell, M., B. F. Jones, and B. A. Olken, 2009, Temperature and Income: Reconciling New Cross-Sectional and Panel Estimates, *American Economic Review* 99, 198–204.

Dell, M., B. F. Jones, and B. A. Olken, 2012, Temperature shocks and economic growth: Evidence from the last half century, *American Economic Journal: Macroeconomics* 4, 66–95.

Dietz, S., and N. Stern, 2015, Endogenous Growth, Convexity of Damage and Climate Risk: How Nordhaus' Framework Supports Deep Cuts in Carbon Emissions, *Economic Theory* 125, 572–620.

Duffie, D., and L. G. Epstein, 1992, Asset Pricing with Stochastic Differential Utility, *Review of Financial Studies* 5, 411–36.

Fischer, T. P., S. Arellano, S. Carn, A. Aiuppa, B. Galle, P. Allard, H. Shinohara T. Lopez, P. Kelly, C. Werner, C. Cardellini, and G. Chiodini, 2019, The emissions of CO_2 and other volatiles from the world's subaerial volcanoes, *Scientific Reports* 9.

Golosov, M., J. Hassler, P. Krusell, and A. Tsyvinsky, 2014, Optimal Taxes on Fossil Fuel in General Equilibrium, *Econometrica* 82, 41–88.

Goodwin, P., 2018, On the time evolution of climate sensitivity and future warming, *Earth's Future* 6, 1336–1348.

Hall, R. E., 1988, Intertemporal Substitution in Consumption, *Journal of Political Economy* 39, 339–347.

Hawkes, A. G., 1971, Spectra of some self-exciting and mutually exciting point processes, *Biometrika* 58, 83–90.

Hayashi, F., 1982, Tobin's Marginal q and Average q: A Neoclassical Interpretation, *Econometrica* 50, 213–224.

Hedin, L. O., 2015, Biogeochemistry: Signs of saturation in the tropical carbon sink, *Nature* 519.

IPCC, 2014, *Fifth Assessment Report of the Intergovernmental Panel on Climate Change* (Cambridge University Press).

Jensen, S., and C. P. Traeger, 2014, Optimal Climate Change Mitigation under Long-term Growth Uncertainty: Stochastic Integrated Assessment and Analytic Findings, *European Economic Review* 69, 104–125.

Jermann, U. J., 1998, Asset Pricing in Production Economies, *Journal of Monetary Economics* 41, 257–275.

Kimball, M. S., and P. Weil, 2009, Precautionary Saving and Consumption Smoothing across Time and Possibilities, *Journal of Money, Credit and Banking* 41l, 245–284.

Knutti, R, and G. C. Hegerl, 2008, The equilibrium sensitivity of the earth's temperature to radiation changes, *Nature Geoscience* 1, 735–743.

Le Quéré, C., C. Roedenbeck, E. T. Buitenhuis, T. J. Conway, R. Langenfelds, A. Gomez, C. Labuschagne, M. Ramonet, T. Nakazawa, N. Metzl, N. Gillett, and M. Heimann, 2007, Saturation of the southern ocean CO_2 sink due to recent climate change, *Science* 316, 1735–1738.

Lemoine, D., and C. P. Traeger, 2016, Economics of tipping the climate dominoes, *Nature Climate Change* 6, 515–519.

McKinsey and Company, 2009, *Pathways to a Low-Carbon Economy: Version 2 of the Global Greenhouse Gas Abatement Cost Curve* (McKinsey and Company, London).

McKinsey and Company, 2010, *Impact of the Financial Crisis on Carbon Economics: Version 2.1 of the Global Greenhouse Gas Abatement Cost Curve* (McKinsey and Company, London).

Meinshausen, M., S. J. Smith, K. V. Calvin, J. S. Daniel, M. L. T. Kainuma, J.-F. Lamarque, K. Matsumoto, S. A. Montzka, S. C. B. Raper, K. Riahi, A. M. Thomson, G. J. M. Velders, and D. van Vuuren, 2011, The RCP greenhouse gas concentrations and their extensions from 1765 to 2300, *Climatic Change* 109.

Moore, F. C., and D. B. Diaz, 2015, Temperature Impacts on Economic Growth Warrant Stringent Mitigation Policy, *Nature Climate Change* 5, 127–131.

Munk, C., and C. Sørensen, 2010, Dynamic asset allocation with stochastic income and interest rates, *Journal of Financial Economics* 96, 433–462.

Nabuurs, G., M. Lindner, P. J. Verkerk, K. Gunia, P. Deda, R. Michalak, and G. Grassi, 2013, First signs of carbon sink saturation in european forest biomass, *Nature Climate Change* 3, 792–796.

Nordhaus, W. D., 1992, An Optimal Transition Path for Controlling Greenhouse Gases, *Science* 258, 1315–1319.

Nordhaus, W. D., 2008, *A Question of Balance: Weighing the Options on Global Warming Policies* (Yale University Press, New Haven).

Nordhaus, W. D., 2017, Revisiting the social cost of carbon, *Proceedings of the National Academy of Sciences* .

Nordhaus, W. D., and P. Sztorc, 2013, DICE 2013R: Introduction and User's Manual, *Technical Report,* Yale University.

Pindyck, R. S., 2011, Modeling the impact of warming in climate change economics, in *The Economics of Climate Change: Adaptations Past and Present*, 47–71 (NBER).

Pindyck, R. S., 2012, Uncertain Outcomes and Climate Change Policy, *Journal of Environmental Economics and Management* 63, 289–303.

Pindyck, R. S., 2013, Climate Change Policy: What Do the Models Tell Us?, *Journal of Economic Literature* 51, 860–872.

Pindyck, R. S., 2014, Risk and Return in the Design of Environmental Policy, *Journal of the Association of Environmental and Resource Economists* 1, 395–418.

Pindyck, R. S., and N. Wang, 2013, The Economic and Policy Consequences of Catastrophes, *American Economic Journal: Economic Policy* 5, 306–339.

Roe, G. H., and M. B. Baker, 2007, Why is climate sensitivity so unpredictable?, *Science* 318, 629–632.

Stern, N., 2007, *The Economics of Climate Change: the Stern Review* (Cambridge University Press).

Tol, R. S. J., 2002a, Estimates on the Damage Costs of Climate Change, Part I: Benchmark Estimates, *Environmental and Resource Economics* 21, 47–73.

Tol, R. S. J., 2002b, Estimates on the Damage Costs of Climate Change, Part II: Dynamic Estimates, *Environmental and Resource Economics* 21, 135–160.

Traeger, C., 2014, A 4-stated DICE: Quantitatively Addressing Uncertainty Effects in Climate Change,, *Environmental and Resource Economics* 59, 1–37.

Traeger, C., 2015, Analytic integrated assessment and uncertainty, *Working Paper* .

van den Bremer, T. S., and F. van der Ploeg, 2019, Pricing Carbon under Economic and Climate Risks: Leading-Order Results from Asymptotic Analysis, *Working Paper* .

van der Ploeg, F., and A. de Zeeuw, 2018, Pricing carbon and adjusting capital to fend off climate catastrophes, *Environmental and Resource Economics* 1–22.

Vissing-Joergenen, A., 2002, Limited Asset Market Participation and the Elasticity of Intertemporal Substitution, *Journal of Political Economy* 110, 825–853.

Vissing-Joergensen, A., and O. P. Attanasio, 2003, Stock-Market Participation, Intertemporal Substitution, and Risk-Aversion, *American Economic Review* 93, 383–391.

Weitzman, M. L., 2012, GHG Targets as Insurance against Catastrophic Climate Damages, *Journal of Public Economic Theory* 14, 221–244.

Williams, S. N., S. J. Schaefer, M. L. Calvache, and D. Lopez, 1992, Global carbon dioxide emission to the atmosphere by volcanoes, *Geochimica et Cosmochimica Acta* 56, 1765–1770.